Structural Characterization of Several $(CO)_3$(dppp)MnX Derivatives, dppp = 1,3-Bis(diphenylphosphino)propane and X = H, OTs, OC_2H_5, Cl, Br, or N_3. An Assessment of Their Efficacy for Catalyzing the Coupling of Carbon Dioxide and Epoxides

Donald J. Darensbourg,* Poulomi Ganguly, and Damon R. Billodeaux

Department of Chemistry, Texas A&M University, College Station, Texas 77843

Received August 19, 2004

The X-ray structures of a series of $(CO)_3$(dppp)MnX complexes, X = H, OTs, OEt, Cl, Br, and N_3, and dppp = 1,3-bis(diphenylphosphino)propane, prepared by literature methods are reported. Several of these derivatives have been examined for their ability to serve as catalysts for the coupling of cyclohexene oxide and carbon dioxide. Although, these organometallic complexes do catalyze the formation of polycarbonate, their activity is not competitive with other very effective catalysts for this coupling reaction. Nevertheless, findings from these studies contribute significantly to our understanding of this important process. The complex containing the alkoxide ligand is the most active, yet it possesses a TON (mol epoxide consumed/mol Mn) of only 50 for a 24 h reaction. In this instance the $(CO)_3$(dppp)MnOEt complex exists as the carbonate species, $(CO)_3$(dppp)MnOC(O)OEt, because of rapid CO_2 insertion into the Mn−OEt bond. The order of epoxide ring-opening by the X group (initiator) was found to be −OC(O)OR > Cl ≥ N_3 > Br. Furthermore, since these complexes are substitutionally inert, this process is best defined as occurring via an associative interchange process and is rate-limiting.

Introduction

The coupling reaction of carbon dioxide and epoxides to provide polycarbonates or cyclic organic carbonate represents one of the most promising reactions for the large-scale utilization of this low-cost C1 feedstock (eq 1).[1] These CO_2-derived products are extremely useful materials, and this synthetic route affords an environmentally benign alternative pathway to their production than that commonly employed.[2] That is, polycarbonates are a class of thermoplastics highly regarded for their optical clarity, exceptional impact resistance, and ductility.[2] Similarly, cyclic organic carbonates are of interest for use in a variety of applications, including high-boiling solvents,[3] additives for hydraulic fluids,[4] and the curing of phenol-formaldehyde resins,[5] plus many more.[6]

The catalytic coupling of CO_2 and epoxides was first reported by Inoue and co-workers in 1969, employing a heterogeneous catalyst derived from $Zn(CH_2CH_3)_2$ and H_2O.[7] More recently, this process has received a great deal of attention utilizing well-defined, more active, homogeneous catalysts.[8] As noted in eq 1, successive ether enchainment leading to polyether linkages in the copolymer is an undesirable reaction that accompanies the completely alternating copolymerization process.

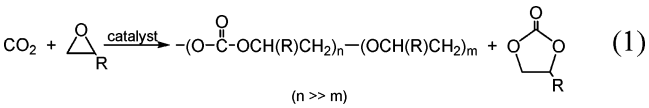

(1)

A fundamental step in the CO_2/epoxide coupling reaction is insertion of carbon dioxide into the metal−alkoxide bond after the epoxide ring-opening process. Indeed, in some instances this insertion reaction can be rate-limiting.[9] Hence, transition metal alkoxides are of particular interest as models in this regard since they

* To whom correspondence should be addressed. Fax: (979) 845-0158. E-mail: djdarens@mail.chem.tamu.edu.

(1) (a) Inoue, S. *Carbon Dioxide as a Source of Carbon*; Aresta, M., Forti, G., Eds.; Reidel Publishing Co.: Dordrecht, 1987; p 331. (b) Darensbourg, D. J.; Holtcamp, M. W. *Coord. Chem. Rev.* **1996**, *153*, 155−174. (c) Rokicki, A.; Kuran, W. *J. Macromol. Sci., Rev. Macromol. Chem.* **1981**, *C21*, 135. (d) Super, M. S.; Beckman, E. J. *Trends Polym. Sci.* **1997**, *5*, 236. (e) For a comprehensive recent review of the area see: Coates, G. W.; Moore, D. R. *Angew. Chem., Int. Ed.* **2004**, in press.

(2) *Engineering Thermoplastics: Polycarbonates, Polyacetals, Polyesters, Cellulose Esters*; Bottenbruch, L., Ed.; Hanson Publishing: New York, 1996; p 112.

(3) Behr, A. *Carbon Dioxide Activation by Metal Complexes*; VCH: Weinheim, 1988; p 7.

(4) Nankee, R. J.; Avery, J. R.; Schrems, J. E. Dow Chem. Patent FR. 15,72,282, 1967; *Chem. Abstr.* **1970**, *72*, 69016p.

(5) Pizzi, H.; Stephanou, A. *J. Appl. Polym. Sci.* **1993**, *49*, 2157.

(6) Shaikh, A.-A. G.; Sivaram, S. *Chem. Rev.* **1996**, *96*, 951−976.

(7) Inoue, S.; Koinuma, H.; Tsuruta, T. *J. Polym. Sci., Part B: Polym. Phys.* **1969**, *7*, 287.

(8) See very recent publications and references therein: (a) Darensbourg, D. J.; Yarbrough, J. C.; Ortiz, C.; Fang, C. C. *J. Am. Chem. Soc.* **2003**, *125*, 7586−7591. (b) Darensbourg, D. J.; Mackiewicz, R. M.; Rodgers, J. L.; Phelps, A. L. *Inorg. Chem.* **2004**, *43*, 1831−1833. (c) Moore, D. R.; Cheng, M.; Lobkovsky, E. B.; Coates, G. W. *Angew. Chem., Int. Ed.* **2002**, *41*, 2599−2602. (d) Moore, D. R.; Cheng, M.; Lobkovsky, E. B.; Coates, G. W. *J. Am. Chem. Soc.* **2003**, *115*, 11911−11924. (e) Eberhardt, R.; Allmendinger, M.; Rieger, M. *Macromol. Rapid Commun.* **2003**, *24*, 194−196. (f) Lu, X.-B.; Wang, Y. *Angew. Chem., Int. Ed.* **2004**, *43*, 3574−3577.

10.1021/om049352v CCC: $27.50
Publication on Web 11/10/2004

undergo insertion of small molecules such as CO_2 or CS_2 into the metal−oxygen bond.[10] For example, Orchin and co-workers have reported the synthesis of octahedral manganese alkoxide complexes of the general formula $(CO)_3$(dppp)MnOR and have examined their ability to reversibily insert CO_2 into the Mn−OR bond to give the corresponding carbonate complexes.[11] In situ infrared spectroscopic kinetic studies by our group showed that the insertion of carbon dioxide into the Mn−OR bond occurred instantaneously at −78 °C via a concerted mechanism.[12] Because of the rapidity of this process, only a lower limit for the second-order constant could be established of 2.0×10^{-3} M^{-1} s^{-1} at −78 °C. This finding prompted us to wonder whether these and other $(CO)_3$(dppp)MnX derivatives could serve as catalysts or catalyst precursors for the CO_2 epoxide coupling reaction. In this report we will present our observations on the subject along with mechanistic implications. Included in this study are the X-ray crystallographically defined structures of these $(CO)_3$(dppp)MnX (X = H, OTs, OC_2H_5, Cl, Br, and N_3) derivatives.

Experimental Section

All syntheses were carried out under argon atmosphere using standard Schlenk and glovebox techniques. Solvents were distilled from appropriate reagents before use. All reagents were commercially available and used without further purification unless otherwise indicated. The synthetic precursors $Mn_2(CO)_{10}$ and 1,3-bis(diphenylphosphino)propane were purchased from Aldrich Chemical Co. Bone dry CO_2 was purchased from Scott Specialty Gases. Infrared spectroscopy were recorded using a Mattson 6021 FTIR spectrometer. ^{1}H NMR spectra were recorded on a 300 MHz Varian Unity Plus spectrometer.

Preparation of *fac*-$(CO)_3$(dppp)MnH (1). The methodology employed in this synthesis was identical to that reported by Orchin and co-workers.[11] X-ray quality crystals were grown by the slow diffusion of hexane to a benzene solution of **1**.

Preparation of *fac*-$(CO)_3$(dppp)MnOTs (2). 2 was synthesized by a previously published procedure.[11] Yellow-orange crystals were obtained from the diffusion of hexane to a concentrated solution of **2** in CH_2Cl_2.

Preparation of *fac*-$(CO)_3$(dppp)MnOC$_2$H$_5$ (3). A 1.0 g (1.72 mmol) sample of *fac*-$(CO)_3$(dppp)MnOCH$_3$ (**3a**), the synthesis of which has already been reported, was slurried with 25 mL of dry ethanol and stirred for 2 h. After 2 h the yellow solid was collected by filtration and washed with 5 mL of hexane.[11] X-ray quality crystals were obtained by slow diffusion of hexane into a concentrated benzene solution of **3**.

Preparation of *fac*-$(CO)_3$(dppp)MnCl (4) and *fac*-$(CO)_3$(dppp)MnBr (5). The syntheses of **4** and **5** have been reported in the literature previously.[13,14] Crystals were grown by slow evaporation of a concentrated CH_2Cl_2 solution of the respective complex into toluene.

Preparation of *fac*-$(CO)_3$(dppp)MnN$_3$ (6). *fac*-[$(CO)_3$(dppp)Mn(OH_2)]BF_4 (**6a**) was synthesized by a previously published procedure.[15] **6a** (0.05 g, 0.1107 mmol) was added with 30 mL of CH_3CN to a suspension of excess NaN_3 in CH_3CN. The mixture was stirred overnight and filtered, and the solvent was removed under reduced pressure. The spectroscopic data agreed with those previously reported.[13] X-ray quality crystals were grown by a slow diffusion of hexane to a CH_2Cl_2 solution of **6**.

X-ray Diffraction Studies. A Bausch and Lomb 10× microscope was used to identify suitable crystals from a representative sample of crystals of the same habit. Crystals were coated with mineral oil, placed on a glass fiber, and mounted on a Bruker SMART 1000 CCD diffractometer. X-ray data were collected covering more than a hemisphere of reciprocal space by a combination of three sets of exposures. Each exposure had a different φ angle for the crystal orientation, and each exposure covered 0.3° in ω. The crystal to detector distance was 4.9 cm. Decay was monitored by repeating collection of the initial 50 frames collected and analyzing the duplicate reflections. Crystal decay was negligible. The space group was determined on the basis of systematic absences and intensity statistics. The structure was solved by direct methods and refined by full-matrix least squares on F^2. All non-hydrogen atoms were refined with anisotropic displacement parameters. All H atoms were placed in idealized positions with fixed isotropic displacement parameters equal to 1.5 times (1.2 for methyl protons) the equivalent isotropic displacement parameters of the atom to which they are attached.

The following programs were used: data collection and cell refinement, SMART;[16] data reduction, SAINTPLUS (Bruker[17]); programs used to solve structures, SHELXS-97 (Sheldrick[18]); programs used to refine structures, SHELXL-99 (Sheldrick[19]); molecular graphics and publication materials, SHELXTL-Plus version 5.0 (Bruker[20]).

Copolymerization of CO_2 and Epoxides. A typical reaction was carried out using the following protocol. A 50 mg sample of the catalyst was dissolved in 20 mL of cyclohexene oxide and injected via inlet port into a Parr autoclave. The reactor was subsequently charged to 500 psi with bone dry CO_2 and stirred at 80 °C for 24 h. After this time the autoclave was cooled and the CO_2 vented in a fume hood. The reactor was opened, and the polymer was isolated by dissolution in small amounts of methylene chloride followed by precipitation from methanol.

Characterization was accomplished by ^{1}H NMR and IR spectroscopy. The amount of ether linkages was determined via ^{1}H NMR by integrating peaks corresponding to the methine protons of the polyether at ∼3.45 ppm and the polycarbonate at ∼4.6 ppm.

Results and Discussion

The syntheses of all of the $(CO)_3$(dppp)MnX complexes utilized in this study have been previously reported in the literature.[11,13−15] Most of these complexes originate from the hydride derivative, $(CO)_3$(dppp)MnH (**1**), which is synthesized via the process depicted in eq 2. Reactions 3−6 indicate the routes to the other Mn(I) complexes of interest. In all instances we were able to find suitable

(9) Darensbourg, D. J.; Mackiewicz, R. M. Billodeaux, D. R. *Organometallics* **2004**, in press.
(10) (a) Darensbourg, D. J.; Sanchez, K. M.; Reibenspies, J. H.; Rheingold, A. L. *J. Am. Chem. Soc.* **1989**, *111*, 7094−7103. (b) Simpson, R. D.; Bergman, R. G. *Angew. Chem., Int. Ed. Engl.* **1992**, *31*, 220. (c) Darensbourg, D. J.; Mueller, B. L.; Bischoff, C. J.; Chojnacki, S. S.; Reibenspies, J. H. *Inorg. Chem.* **1991**, *30*, 2418−2424.
(11) Mandel, S. K.; Ho, D. M.; Orchin, M. *Organometallics* **1993**, *12*, 1714−1719.
(12) Darensbourg, D. J.; Lee, W.-Z.; Phelps, A. L.; Guidry, E. *Organometallics* **2003**, *22*, 5585−5588.
(13) Li, G. Q.; Feldman, J. *Polyhedron* **1997**, *16*, 2041−2045.
(14) Riera; V. *J. Organomet. Chem.* **1981**, *205*, 371−379.
(15) Becker, T. M.; Orchin, M. *Polyhedron* **1999**, *18*, 2563−2571.
(16) *SMART 1000 CCD*; Bruker Analytical X-ray Systems: Madison, WI, 1999.
(17) *SAINT-Plus*, version 6.02; Bruker: Madison, WI, 1999.
(18) Sheldrick, G. *SHELXS-97*: Program for Crystal Structure Solution; Institut fur Anorganische Chemie der Universitat: Gottingen, Germany, 1997.
(19) Sheldrick, G. *SHELXL-99*: Program for Crystal Structure Refinement; Institut fur Anorganische Chemie der Universitat: Gottingen, Germany, 1999.
(20) *SHELXTL*, version 5.0; Bruker: Madison, WI, 1999.

Table 1. Crystallographic Data and Data Collection Parameters for Complexes 1−6

	1	2	3	4	5	6
empirical formula	$C_{30}H_{27}MnO_3P_2$	$C_{37}H_{33}MnO_6P_2S$	$C_{32}H_{31}MnO_4P_2$	$C_{30}H_{26}ClMnO_3P_2$	$C_{30}H_{26}BrMnO_3P_2$	$C_{30}H_{26}N_3MnO_3P_2$
cryst syst	triclinic	monoclinic	triclinic	monoclinic	monoclinic	monoclinic
space group	$P\bar{1}$	$P2(1)/n$	$P\bar{1}$	$P2(1)/n$	$P2(1)/n$	$P2(1)/c$
volume (Å^3)	2634.3(15)	3385.7(17)	1443.7(12)	2696.8(8)	2739.4(19)	3208.7(12)
a (Å)	11.017(4)	10.539(3)	7.921(4)	9.9382(18)	10.073(4)	12.826(3)
b (Å)	15.451(5)	14.793(4)	10.031(5)	20.643(3)	20.612(8)	17.209(4)
c (Å)	15.773(5)	21.716(6)	18.271(9)	13.666(3)	13.765(6)	15.102(3)
α (deg)	95.888(6)	90	94.634(8)	90	90	90
β (deg)	90.886(6)	90.534(5)	93.541(9)	105.871(3)	106.551(7)	105.727(4)
γ (deg)	99.3047(7)	90	91.340(9)	90	90	90
temperature (K)	110(2)	110(2)	110(2)	110(2)	273(2)	110(2)
d_{calc} (g/cm^3)	1.393	1.418	1.372	1.445	1.531	1.39
Z	4	4	2	4	4	4
μ (mm^{-1})	0.653	0.592	0.604	0.738	2.088	0.552
no. of reflns collected	11 907	14 890	6428	12 136	12 140	14 172
no. of indep reflns	7558	4885	4098	3879	3954	4611
no. of params	657	425	353	334	334	406
goodness-of-fit on F^2	1.051	1.094	1.043	0.968	1.159	1.08
final R indices [$I>2\sigma(I)$]	R_1= 0.0798	R_1= 0.0382	R_1= 0.0726	R_1= 0.0730	R_1= 0.0598	R_1= 0.0623
R indices (all data)	wR_2= 0.1078	wR_2= 0.0437	wR_2= 0.1017	wR_2=0.1430	wR_2= 0.0737	wR_2= 0.0875

conditions to obtain crystalline samples for carrying out X-ray crystallographic studies of these derivatives.

$$Mn_2(CO)_{10} + dppp \xrightarrow{C_3H_7OH} \underset{\mathbf{1}}{(CO)_3(dppp)MnH} \quad (2)$$

$$\mathbf{1} + p\text{-}TsOH \rightarrow \underset{\mathbf{2}}{(CO)_3(dppp)MnOTs} \xrightarrow{NaOCH_3} \quad (3)$$

$$\underset{\mathbf{3a}}{(CO)_3(dppp)MnOCH_3} \xrightarrow{C_2H_5OH} \underset{\mathbf{3}}{(CO)_3(dppp)MnOC_2H_5}$$

$$\mathbf{1} + CCl_4 \rightarrow \underset{\mathbf{4}}{(CO)_3(dppp)MnCl} \quad (4)$$

$$BrMn(CO)_5 + dppp \rightarrow \underset{\mathbf{5}}{(CO)_3(dppp)MnBr} \quad (5)$$

$$\mathbf{1} + HBF_4{\cdot}Et_2O \rightarrow$$

$$\underset{\mathbf{6a}}{[(CO)_3(dppp)Mn(OH_2)]BF_4} \xrightarrow{NaN_3} \underset{\mathbf{6}}{(CO)_3(dppp)MnN_3} \quad (6)$$

The structures of molecules **1**−**6** are indicative of a manganese atom octahedrally coordinated to three (*facial*) terminal carbonyl groups, a chelating 1,3-bis(diphenylphosphino)propane (dppp) ligand, and a nucleophile (X). The latter group is *trans* to one carbonyl and has a *cis* orientation to the remaining two carbonyls as well as the chelating ligand, as has been observed by Orchin and co-workers for one such derivative.[11] Table 1 contains crystallographic and structure refinement data for complexes **1**−**6**. All thermal ellipsoid drawings are at 50% probability, and in general the hydrogen atoms have been omitted for clarity, with the notable exception of the hydride in complex **1**. The relevant bond distances and bond angles based on the atomic numbering scheme in these figures are listed in Table 2. The molecular structure of **1** is provided in Figure 1. Complex **1** crystallized in the space group $P\bar{1}$ with two molecules in the asymmetric unit. The position of the hydrogen atom was located by a difference map to define the average Mn−H bond length of 1.72 Å.

Table 2. Selected Bond Lengths (Å) and Angles (deg) for Complexes 1−6

	Complex **1**		
Mn(1A)−H(1A)	1.735(19)	Mn(1A)−C(1A)	1.8120(6)
Mn(1A)−P(1A)	2.2881(18)	Mn(1A)−C(2A)	1.837(6)
Mn(1A)−P(2A)	2.2927(17)	Mn(1)−C(3A)	1.814(7)
P(2A)−Mn−P(1A)	89.42		
C(2A)−Mn−H(1A)	175.4(19)		
Mn(1B)−H(1B)	1.71(6)	Mn(1B)−C(1B)	1.814(7)
Mn(1B)−P(1B)	2.3047(16)	Mn(1)−C(2B)	1.809(5)
Mn(1B)−P(2B)	2.2828(18)	Mn(1)−C(3B)	1.812(6)
P(2B)−Mn−P(1B)	89.42		
C(2B)−Mn−H(1B)	175.4(19)		
	Complex **2**		
Mn(1)−O(1)	2.092(2)	Mn(1)−C(27)	1.774(3)
O(1)−S(1)	1.495(2)	Mn(1)−C(26)	1.833(3)
S(1)−O(2)	1.439(2)	Mn(1)−C(36)	1.834(3)
S(1)−O(3)	1.431(2)		
S(1)−C(28)	1.769(3)		
C(26)−Mn(1)−O(1)	178.27(11)	O(1)−S(1)−C(28)	102.78(12)
O(3)−S(1)−O(2)	115.42(14)		
	Complex **3**		
Mn(1)−O(4)	2.037(3)	Mn(1)−C(1)	1.841(7)
O(4)−C(31)	1.394(7)	Mn(1)−C(2)	1.832(6)
C(31)−C(32)	1.534(8)	Mn(1)−C(3)	1.789(6)
C(31)−O(4)−Mn(1)	117.7(3)		
P(1)−Mn(1)−P(2)	90.54(6)		
	Complex **4**		
Mn(1)−Cl(1)	2.379(2)	Mn(1)−C(3)	1.802(9)
Mn(1)−C(1)	1.814(9)		
Mn(1)−C(2)	1.754(9)		
C(2)−Mn−Cl(1)	174.9(3)		
	Complex **5**		
Mn(1)−Br(1)	2.5189(11)	Mn(1)−C(3)	1.821(6)
Mn(1)−C(1)	1.816(6)		
Mn(1)−C(2)	1.783(6)		
C(2)−Mn−Br(1)	174.02(17)		
	Complex **6**		
Mn(1)−N(1)	2.126(3)	Mn(1)−C(1)	1.816(5)
N(1)−N(2)	1.164(5)	Mn(1)−C(2)	1.832(5)
N(2)−N(3)	1.200(6)	Mn(1)−C(3)	1.799(5)
N(2)−N(1)−Mn(1)	117.2(3)		
N(1)−N(2)−N(3)	175.4(4)		

Complex **2**, (CO)$_3$(dppp)MnOTs, crystallized in the space group $P2_1/n$. A thermal ellipsoid representation of **2** is shown in Figure 2. Selected bond distances and bond angles are tabulated in Table 2. Notably, the Mn−tosylate bond length was found to be 2.092(2) Å, with the tosylate S(1)−O(1) bond distance of 1.495(2)Å being

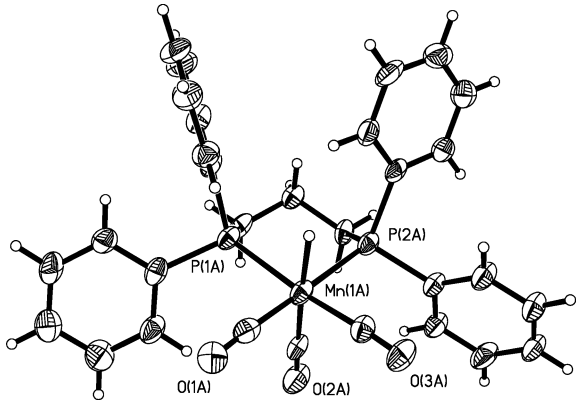

Figure 1. Thermal ellipsoid representation of *fac*-$(CO)_3$(dppp)MnH, **1**.

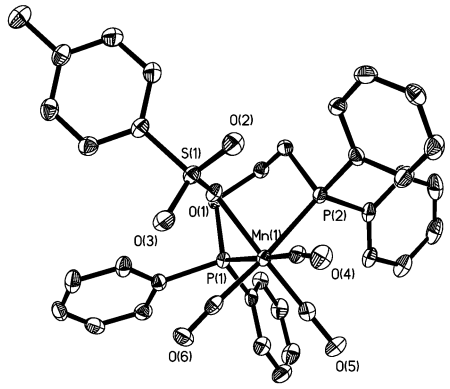

Figure 2. Thermal ellipsoid representation of *fac*-$(CO)_3$(dppp)MnOTs, **2**.

slightly longer than the S(1)−O(2) and S(1)−O(3) distances, which average 1.435 Å. The sulfur−phenyl ring (S(1)−C(28)) bond length was determined to be 1.769(3) Å. As expected, the two types of carbonyl ligands have different Mn−C distances, with the $Mn-CO_{axial}$ bond length of 1.774(3) Å shorter than the $Mn-CO_{eq}$ average distance of 1.833(3) Å.

We were extremely fortunate to isolate in crystalline form and characterize via X-ray crystallography the $(CO)_3$(dppp)MnX derivative where X = ethoxide. In general the alkoxide group in the absence of electron-withdrawing substituents affords complexes that are extremely reactive toward trace quantities of CO_2 in the atmosphere even in the solid state.[12] Typically, these derivatives are characterized in the solid state as their CO_2-inserted product. For example, the structure of the methoxide analogue of **3** was reported as its alkoxycarbonate derivative, $(CO)_3$(dppp)MnOC(O)OCH_3.[11] Complex **3** crystallized in the triclinic space group $P\bar{1}$. The Mn−O bond distance of 2.037(3) Å compares favorably to the Mn−O bond distance of 2.029(3) Å observed in the *fac*-$(CO)_3$(dppp)MnOC(O)OCH_3 derivative.[11] As was observed in complex **2**, the $Mn-CO_{axial}$ bond length of 1.789(6) Å is significantly shorter than the $Mn-CO_{eq}$ distance of 1.841(7) Å. A thermal ellipsoid representation of **3** is provided in Figure 3.

The halide derivatives, complexes **4** and **5**, crystallized in the monoclinic space group $P2_1/n$. The Mn−Cl bond length in **4** of 2.379(2) Å is comparable to that seen in the closely related derivative, *fac*-$(CO)_3$(depe)MnCl, of 2.406(2) Å.[11] The Mn−Br bond length in complex **5** of 2.518(9) Å is as expected on the basis of the difference

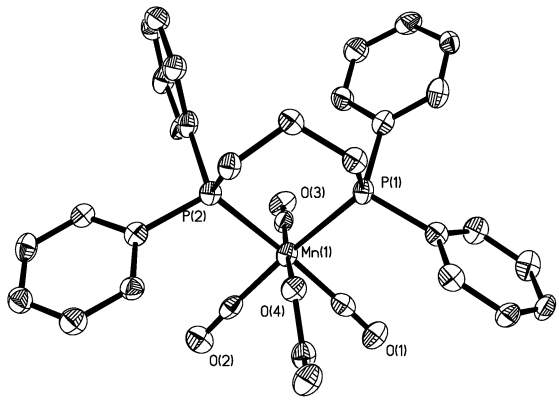

Figure 3. Thermal ellipsoid representation of *fac*-$(CO)_3$(dppp)$MnOC_2H_5$, **3**.

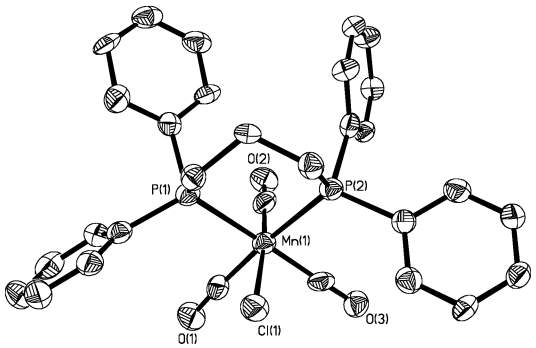

Figure 4. Thermal ellipsoid representation of *fac*-$(CO)_3$(dppp)MnCl, **4**.

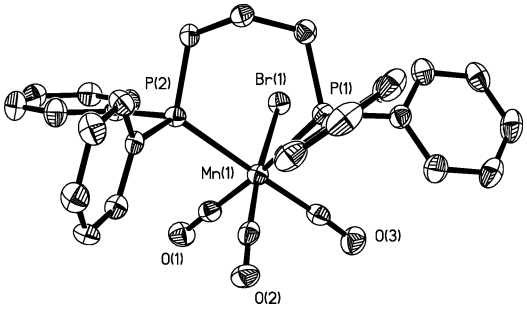

Figure 5. Thermal ellipsoid representation of *fac*-$(CO)_3$(dppp)MnBr, **5**.

in the covalent radii of 0.15 Å of the two halogen atoms. Unlike complex **3**, these manganese derivatives are very air stable. Figures 4 and 5 depict the thermal ellipsoid representations of complexes **4** and **5**.

In our studies involving the use of (salen)$Cr^{III}X$ (X = Cl or N_3) complexes as catalysts for the effective coupling of CO_2 and epoxides to afford polycarbonates, the azide derivatives were found to be better initiators than their chloride analogues.[8b,21] Hence, it was of importance to obtain a well-characterized sample of $(CO)_3$(dppp)MnN_3 for our current studies. This was achieved via reaction of the aquo complex, [$(CO)_3$(dppp)-$Mn(OH_2)$][BF_4], with an aqueous solution of NaN_3. $(CO)_3$(dppp)MnN_3 (**6**) crystallized in the space group $P2_1/c$ as a benzene solvate. A thermal ellipsoid drawing of complex **6** is found in Figure 6, along with the atomic

(21) Darensbourg, D. J.; Mackiewicz, R. M.; Rodgers, J. L.; Fang, C. C.; Billodeaux, D. R.; Reibenspies, J. H. *Inorg. Chem.* **2004**, *43*, 6024−6034.

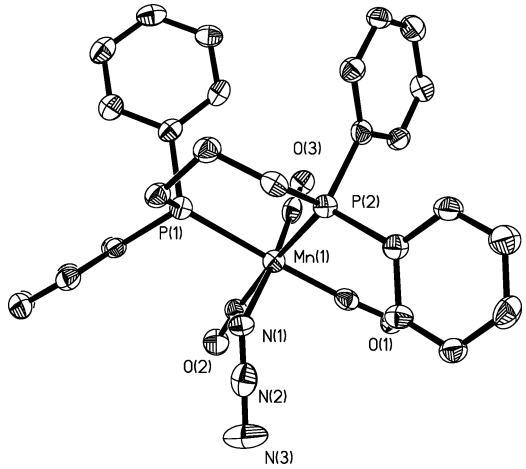

Figure 6. Thermal ellipsoid representation of *fac*-(CO)$_3$-(dppp)MnN$_3$, **6**.

Table 3. ν_{CO} Stretching Vibrations in (CO)$_3$(dppp)MnX Complexes[a]

X	ν_{CO}, cm^{-1}	average ν_{CO}, cm^{-1}
H (**1**)	1998, 1926, 1902	1942
OTs (**2**)	2037, 1969, 1911	1972
OC_2H_5 (**3**)	2009, 1936, 1891	1945
Cl (**4**)[b]	2027, 1957, 1905	1963
Br (**5**)	2028, 1963, 1908	1966
N_3 (**6**)	2014, 1956, 1912	1960

[a] Spectra determined in benzene solution. [b] Spectrum determined in dichloromethane.

numbering scheme for selected atoms. The Mn−azide bond distance was found to be 2.126(3) Å, and the nearly linear N_3 unit (175.4(4)°) formed an angle with the Mn−N(1) bond of 117.2(2)°. Bond distances within the azide ligand are N(1)−N(2) = 1.164(5) Å and N(2)−N(3) = 1.200(6) Å.

An interesting feature of the Mn^{I}−azide linkage in complex **6** as compared to that in (salen)Cr^{III} azides is the internal nitrogen−nitrogen bond distances.[9] Considering the

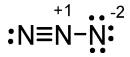

resonance form for the free azide moiety, in the low-valent manganese derivative the azide ligand binds via the triply bonded terminal nitrogen, whereas in the chromium(III) salen derivative it binds through the terminal single-bonded nitrogen atom. That is, in the six-coordinate chromium salen complex, N(1)−N(2) = 1.210(9) Å and N(2)−N(3) = 1.144(8) Å. This difference in binding modes might be anticipated on the basis of hard/soft arguments. On the other hand, the ν_{asym} mode for complex **6** is observed at 2056 cm^{-1}, whereas that of the chromium(III) azide complex is similarly found at 2054 cm^{-1}.

Table 3 lists the ν_{CO} values for the manganese derivatives described in this report. These ν_{CO} stretching vibrations reflect the electron density available at the metal center for back-bonding to the carbonyl ligands. Therefore, it is possible from the average ν_{CO} frequency for these six derivatives to order the electron-rich character of the metal centers as **1** ≥ **3** > **6** > **4** = **5** > **2**. This will be useful information when considering these complexes as catalysts for the coupling of CO_2 and epoxides.

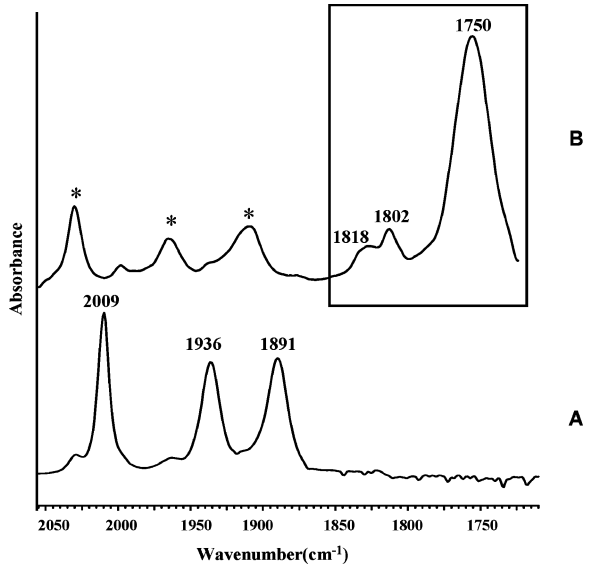

Figure 7. Infrared spectra in the ν_{CO} and ν_{CO_2} regions before and after CO_2/cyclohexene oxide coupling reaction. (A) ν_{CO} of (CO)$_3$(dppp)MnOC$_2$H$_5$; (B) ν_{CO} and ν_{CO_2} of (*)(CO)$_3$(dppp)MnOC(O)OC$_2$H$_5$, (1818, 1802) *trans*-cyclic carbonate and (1750 cm^{-1}) poly(cyclohexylene)carbonate.

Scheme 1

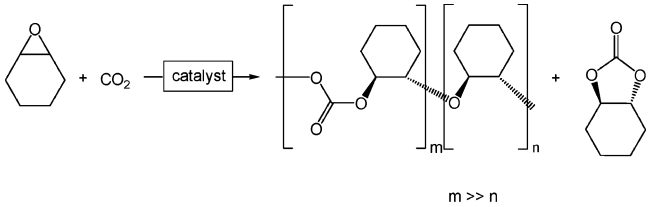

The complexes (CO)$_3$(dppp)MnX (X = OCH_3, OC_2H_5 (**3**), Cl (**4**), Br (**5**), and N_3 (**6**)) were examined for their efficacy for catalyzing the coupling of cyclohexene oxide and carbon dioxide (Scheme 1). Reaction conditions were consistent with those we routinely employ for the very effective (salen)CrX/cocatalyst systems, i.e., catalyst loading 0.040 mol %, 500 psi CO_2 pressure, and 80 °C. After a polymer run the crude reaction mixture was dissolved in methylene chloride and examined by infrared spectroscopy for product identification. Importantly, in these instances the highly informative metal carbonyl absorbances in the infrared also provide a probe of the resting state of the catalytically active species. Figure 7 represents the infrared spectra in the carbonyl region of the before and after reaction solutions for the copolymerization process involving the most effective catalyst examined here, complex **3**. As is evident in Figure 7, the major reaction product is the poly(cyclohexylene)carbonate, with a minor quantity of the *trans*-cyclohexyl carbonate also afforded. That is, the ν_{CO_2} bond at 1750 cm^{-1} corresponds to the copolymer carbonate function, with the weak absorbances at 1802 and 1818 cm^{-1} to that of the *trans* cyclic carbonate.[22] The ν_{CO} absorbances at 2029, 1962, and 1903 cm^{-1} are readily assigned to the CO stretching vibrations of the (CO)$_3$(dppp)Mn−OC(O)OR species, where R represents the growing polymer chain. This assignment is greatly aided by comparison with the fully characterized (CO)$_3$-

(22) Darensbourg, D. J.; Lewis, S. J.; Rodgers, J. L.; Yarbrough, J. C. *Inorg. Chem.* **2003**, *42*, 581−589.

Table 4. Results of Mn^I Complexes-Catalyzed Coupling Reactions of Cyclohexene Oxide and CO_2[a]

	TON[b]		
catalyst	copolymer	cyclic carbonate	% carbonate
$(CO)_3$(dppp)$MnOCH_3$	42	11	66
$(CO)_3$(dppp)$MnOC_2H_5$	40 (48)[c]	10 (25)[c]	70 (83)[c]
$(CO)_3$(dppp)MnCl	30 (44)[c]	10 (28)[c]	56 (72)[c]
$(CO)_3$(dppp)MnN_3	24	10	47
$(CO)_3$(dppp)MnBr	12	8	25

[a] Reactions carried out for 24 h at 80 °C. [b] Mol of epoxide consumed/mol of Mn. [c] Reactions carried out at 100 °C.

(dppe)MnOC(O)OMe derivative previously reported.[11,12] As expected, a similar spectrum in the ν_{CO} region is observed at the end of the copolymerization reaction for all of the manganese catalysts employed in Table 4. Furthermore, this species would be expected to be the resting state of the catalyst on the basis of the very facile insertion of CO_2 into the Mn−OMe bond of $(CO)_3$(dppe)-MnOMe.[12]

Table 4 summarizes the results of the CO_2/cyclohexene oxide coupling reaction catalyzed by the Mn^I derivatives reported herein. Although these organometallic complexes do serve as catalysts for this process, the TONs for 24 h runs are not very impressive relative to other catalysts for this reaction. For example, the best catalysts found in this study were those containing alkoxide initiators, yet these exhibited TONs only around 50 mol epoxide consumed/mol Mn with 70% carbonate linkages at 80 °C. Concomitantly, the selectivity for copolymer production was only 80%; that is, the minor product, *trans*-cyclohexyl carbonate, accounts for 20% of the coupling product. As anticipated, an increase in reaction temperature to 100 °C increased the percentage of cyclic carbonate formation to about 34%; however, the higher temperature favorably enhanced both the TON and % carbonate linkages in the copolymer.

Concluding Remarks

Herein we have structurally characterized a series of closely related 18-electron derivatives of $(CO)_3$(dppp)-MnX, which differ only in the nature of the X group. Although these complexes were found not to be very effective catalysts for the coupling of CO_2 and epoxides, findings from these studies contribute significantly to our understanding of this important process. Furthermore, these complexes have previously been shown via ^{13}CO exchange studies to be thermally inert to ligand dissociation.[12] Hence, upon utilizing these derivatives as catalysts for the CO_2/epoxide coupling reaction, ring-opening of the epoxide must be taking place via an associative interchange mechanism. Because CO_2 insertion into the Mn^I−OR bond in the absence of electron-withdrawing substituents on R has been shown to be rapid even at −78 °C, in the presence of CO_2 the $(CO)_3$(dppp)MnOR (R = Me, Et) complexes will exist as $(CO)_3$(dppp)MnOC(O)OR (R = Me, Et).[12]

Scheme 2

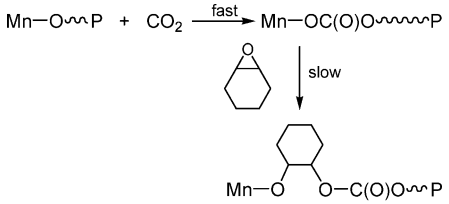

P = growing polymer chain

As the data in Table 4 indicate, the order of epoxide ring-opening by the X group (initiator) is −OC(O)OR > Cl ≥ N_3 > Br. This trend roughly parallels what is observed in the (salen)CrX-catalyzed processes, as well as the electron-donating abilities of the X groups as revealed by their effect on the ν_{CO} values of the Mn^I carbonyl derivatives. The observation that *trans*-cyclohexyl carbonate is selectively produced is consistent with it being formed by copolymer degradation.[23] Consequently, cyclic carbonate production should be independent of the initiator, which is borne out by the data in Table 4. The somewhat reduced cyclic carbonate production in the case of X = Br is undoubtedly due to the significant reduction in copolymer production in this instance. Furthermore, the enhanced production of cyclic carbonate over copolymer at higher reaction temperatures is consistent with a unimolecular degradation of the growing polymer chain.[8a] In our previous studies involving (salen)CrX derivatives as catalysts for this process we have noted that at the onset of the copolymerization process larger amounts of polyether linkages are seen in the copolymer, which upon longer reaction times afford copolymers with >99% carbonate content. This observation would account for the large degree of polyether linkages, i.e., the small degree of carbonate linkages in the slowly initiating bromide derivative.

Hence, these studies reinforce the proposed mechanistic features of the more complex (salen)CrX/cocatalyst systems.[21] However, in this instance unlike in the (salen)CrX/cocatalyst system,[9] CO_2 insertion into the alkoxide intermediate under all reaction conditions is faster than epoxide ring-opening by the transient carbonate moiety of the growing polymer chain (Scheme 2). That is, the rate-limiting step in the propagation process of the copolymerization reaction is epoxide ring-opening and not CO_2 insertion.

Acknowledgment. Financial support from the National Science Foundation (CHE 02-34860) and the Robert A. Welch Foundation is greatly appreciated.

Supporting Information Available: Complete details for the crystallographic study of complexes **1**−**6**. This material is available free of charge on the Internet at http://pubs.acs.org.

OM049352V

(23) Darensbourg, D. J.; Fang, C. C.; Rodgers, J. L. *Organometallics* **2004**, *23*, 924−927.